SCIENTIFIC REP**O**RTS

OPEN

All optical dual stage laser wakefield acceleration driven by two-color laser pulses

Vishwa Bandhu Pathak [1], Hyung Taek Kim [1,2], J. Vieira [3], L. O. Silva [3] & Chang Hee Nam[1,4]

We propose an all-optical dual-stage laser wakefield acceleration (LWFA), staged with co-propagating two-color laser pulses in a plasma medium, to enhance the electron bunch energy. After the depletion of the leading fundamental laser pulse that initiates self-injection and sets up the first stage particle acceleration, the subsequent second-harmonic laser pulse takes over the acceleration process and accelerates the electron bunch in the second stage over a significantly longer distance than in the first stage. In this all optical dual-stage LWFA, the electrons can gain 3 times higher energy as compared to the energy gain from the single stage LWFA driven by a single-color laser pulse with equivalent energy. Our multi-dimensional particle-in-cell simulations demonstrate that a 10-GeV electron bunch with 20-pC charge can be obtained by the two-color dual-stage LWFA using total input laser power of 0.6 PW.

Laser-plasma electron acceleration[1–5] is a promising approach to the next generation of electron accelerators because it can provide an accelerating field that can be more than three orders of magnitude larger than those of conventional devices. The progress of high power laser technologies[6,7] and theoretical expectations[8,9] have stimulated conceptual designs to realize an electron accelerator with energy over 100 GeV based on laser wakefield acceleration (LWFA)[10]. The radial ponderomotive force associated with a short and intense laser pulse can lead to the cavitation of all plasma electrons from the region where the laser pulse propagates, creating a spherical plasma wave (bubble or blowout[11,12]). The large accelerating field associated with the blowout can trap and accelerate plasma electrons (self-injection), or positrons if a Laguerre-Gaussian laser beam is used as a driver[13].

In LWFA, the acceleration length is one of the important parameters determining the final electron energy. For a self-guided laser pulse[14], the effective acceleration length is limited either by the laser etching (depletion) length $[L_{etch} \approx (\omega_0/\omega_p)^2 c \tau_L]$[9], or by the dephasing length $[L_d = (4/3)(\omega_0^2/\omega_p^2)\sqrt{a_0}\, c/\omega_p]$[9], where $a_0 = eE_0/(m_e c \omega_0)$ is the normalized vector potential of the laser, c is the speed of light in vacuum, and E_0, ω_0 and τ_L are the peak laser electric field, laser central frequency and laser pulse length respectively. In addition, $\omega_p = \sqrt{4\pi n_0 e^2/m}$ is the plasma frequency with n_0 being plasma density, and m, e electron rest mass and elementary charge, respectively. As it is clear from the expressions above, the acceleration length, and thus the energy gain, is higher at lower plasma densities because the ratio ω_0/ω_p is higher. In contrast, particle trapping is easily met at higher plasma densities, because the required longitudinal electron momentum for self-injection also scales with ω_0/ω_p. Therefore, the electron injection and the acceleration length are the competing factors in the optimization of plasma density for LWFA in single stage.

In order to solve this problem, dual-stage LWFA[10,15–19] has been proposed with a short, high density plasma in the first stage (injector stage) and a long, low density plasma in the second stage (accelerator stage). The dual-staged LWFA can be achieved either by a single laser pulse propagating through two plasma media[16,20–22] or by two independent laser pulses focused separately to two plasma media[15,18,19]. All these methods for dual-staged LWFA require two plasma media with Luo et al.[19] showing multi stage coupling of LWFA in curved plasma channel from 2D PIC simulations using OSIRIS[23,24].

Manipulating the laser frequency to realize a multi-stage LWFA is considerably more challenging. There are growing interests on all-optical control of LWFA, by manipulating optical properties of driving laser pulse[25–27] or

[1]Center for Relativistic Laser Science, Institute for Basic Science (IBS), Gwangju, 61005, Korea. [2]Advanced Photonics Research Institute, Gwangju Institute of Science and Technology (GIST), Gwangju, 61005, Korea. [3]GoLP/Instituto de Plasmas e Fusão Nuclear, Instituto Superior Técnico, Universidade de Lisboa, Lisbon, Portugal. [4]Department of Physics and Photon Science, GIST, Gwangju, 61005, Korea. Correspondence and requests for materials should be addressed to H.T.K. (email: htkim@gist.ac.kr) or C.H.N. (email: chnam@gist.ac.kr)

by composing multiple laser pulses[28–31]. While the frequency chirp approach can be employed to control injection and acceleration[27], it is severely limited by the maximum chirp that may be introduced in a single laser pulse driver. Here we explore an innovative solution to this limitation by proposing to use a two-color laser pulse to create the injector and accelerator stage in a single homogeneous plasma column. In our proposed model, the leading pulse, at the fundamental frequency, acts as an injector and the trailing laser pulse, at the second harmonic, works as an accelerator or booster. We derived an analytical expression for the energy scaling of all-optical dual stage LWFA in the matched regime[9,12]. Using PIC simulations with OSIRIS[23,24], we demonstrate the proof-of-principle of this concept to achieve quasi-mono-energetic multi-GeV electron bunch in 3D calculations and the generation of 10-GeV electron beam by two-color laser pulses having the input laser power of 0.6 PW in 2D calculations.

Results

Energy gain in all optical dual-stage LWFA. The two-color dual-stage LWFA can be understood as following: In the injector stage, the leading lower frequency laser pulse excites a plasma wave with a lower phase velocity, which triggers electron self-injection (injector stage). The second harmonic laser pulse, trailing just behind the leading pulse, is guided within the bubble. The second harmonic laser will drive wakefields once the leading pulse depletes. These wakefields move faster than those of the injector stage, being ideal to boost the energy of the self-injected electrons. This is the acceleration stage. The transition from the injection stage to the acceleration stage is regulated by the temporal delay between the two color laser pulses. We show that, by fine-tuning the time delay between the two-color laser pulses, quasi-mono-energetic features can be obtained in the accelerated electron beam.

To estimate the energy gain of the two-color dual-stage LWFA, let us consider a fundamental frequency laser pulse (FL) with normalized vector potential $a_{0(\omega_0)}$, frequency ω_0, spot-size $W_{0(\omega_0)}$ and pulse duration $\tau_{L(\omega_0)}$ is propagating in a homogeneous plasma with density n_0. The FL is followed by a second harmonic laser pulse (SL) with time delay t_d with respect to FL, normalized vector potential $a_{0(2\omega_0)}$, frequency $2\omega_0$, spot-size $W_{0(2\omega_0)}$ and pulse duration $\tau_{L(2\omega_0)}$. The length of the first stage of LWFA led by the FL is limited to $L_{s1} = c\tau_{L(\omega_0)}\omega_0^2/\omega_p^2$ because of localized etching[32], which is also close to the dephasing length in the matched regime[9]. Assuming that the trailing SL does not significantly influence the bubble evolution in the first stage, the energy gain in the first stage is given by $\Delta E_{s1} = \left(\frac{2}{3}\right)mc^2 a_{0(\omega_0)}^2 \omega_0^2/\omega_p^2$. Once the leading laser pulse is absorbed, the SL takes over the wakefield excitation in the accelerator stage characterized by 4 times longer etching length as compared to the first stage. Since the acceleration length in the second stage is expected to be limited by the dephasing, the acceleration length of the second stage can be given as $L_{s2} = (8/3)\omega_0^2/\omega_p^2 R$, where $R = 2\sqrt{a_{0(2\omega_0)}}$[9] is the bubble radius. Hence, the energy gain in the second stage can be written as $\Delta E_{s2} = (8/3)\,mc^2 a_{0(2\omega_0)}\omega_0^2/\omega_p^2$ and the total energy gain can be estimated as,

$$\Delta E = \frac{2}{3}mc^2\frac{\omega_0^2}{\omega_p^2}a_{0(\omega_0)}\left(1 + 4\frac{a_{0(2\omega_0)}}{a_{0(\omega_0)}}\right).$$

(1)

For total input power $P_{in} = P_{\omega_0} + P_{2\omega_0}$ with the FL power, P_{ω_0}, the SL power, $P_{2\omega_0}$, and the second harmonic conversion efficiency $\alpha = P_{2\omega_0}/P_{in}$, we can re-write Eq. (1) as:

$$\Delta E[\text{GeV}] = 1.7\,G_d\left(\frac{P_{in}[\text{TW}]}{100}\right)^{\frac{1}{3}}\left(\frac{10^{18}}{n_0[\text{cm}^{-3}]}\right)^{\frac{2}{3}}\left(\frac{0.8}{\lambda_0[\mu m]}\right)^{\frac{4}{3}},$$

(2)

where $G_d = (1 - \alpha)^{1/3} + 2^{4/3}\alpha^{1/3}$ is the extra gain provided by the dual stage acceleration. For $\alpha = 0.05$ to 0.9, G_d slowly varies from 2.0 to 3.0, providing a stable gain factor. For $\alpha = 0$, $G_d = 1$ and the energy scales same as in Lu et al.[9]. However, for the same total laser input power our proposed scheme can significantly enhance the acceleration gain by a factor in the range between 2 to 3. As a result, the two-color laser pulses with $P_{in} = 1$ PW, nowadays available from a PW laser facility, can produce 10-GeV electron bunches for $\alpha = 0.3$.

Proof of principle simulation. In order to show the feasibility of the all-optical dual stage LWFA, a set of multi-dimensional PIC simulations are performed using OSIRIS[23,24]. We consider two-color laser pulses of input laser power 215 TW propagating in a 0.7-cm plasma with density $7.75 \times 10^{18}\,\text{cm}^{-3}$. We initialize a simulation box, which moves with the speed of light c, has dimensions of $25\,c/\omega_p \times 30\,c/\omega_p \times 30\,c/\omega_p$ and are divided into $3000 \times 280 \times 280$ cells, along z, x and y direction respectively, with 2 particles per cell. The FL with frequency $\omega_0 = 15\,\omega_p$ is initialized with parameters: $a_{0(\omega_0)} = 8$, $W_{0(\omega_0)} = 6\,c/\omega_p$ and $\tau_{L(\omega_0)} = \frac{\lambda_p}{2} = 3.14\,\omega_p^{-1}$, and the SL with frequency $2\,\omega_0$ and $\alpha = 0.3$ is initialized in the simulation box at a distance $4.5c/\omega_p$ away from the leading pulse with parameters $a_{0(2\omega_0)} = 4$, $W_{0(2\omega_0)} = 4\,c/\omega_p$ and $\tau_{L(2\omega_0)} = \frac{\lambda_p}{2}$. The plasma is initialized just in front of the leading pulse, with an initial density ramp of size $100\,c/\omega_p$ and then a constant homogeneous plasma density.

The 3D PIC simulations demonstrate that two-color laser pulses can realize the dual-stage acceleration. The results obtained from the 3D simulation is shown in Fig. 1, where panels (a)-(e) plot the laser fields for FL and SL, and the corresponding electron density distribution in the y-z simulation plane at various stages of the acceleration process, and panels (f)-(j) show the corresponding electron distribution in phase space. The panels (a) and (f) demonstrate the excitation of bubble, self-injection by FL, and the guiding of SL inside the bubble in the first stage. The panels (b) and (g) show the depletion of leading FL and the initial onset of the second stage by the SL. Panels (c) and (h) clearly show the coupling of the electron bunch, from the first stage to the second stage. An electron beam with 2nC charge in 500–600 MeV energy was injected into the second stage with 12 mrad divergence and 16 mm mrad emittance, and further accelerated to 1.5 GeV with 0.3 nC charge above 1 GeV, as shown
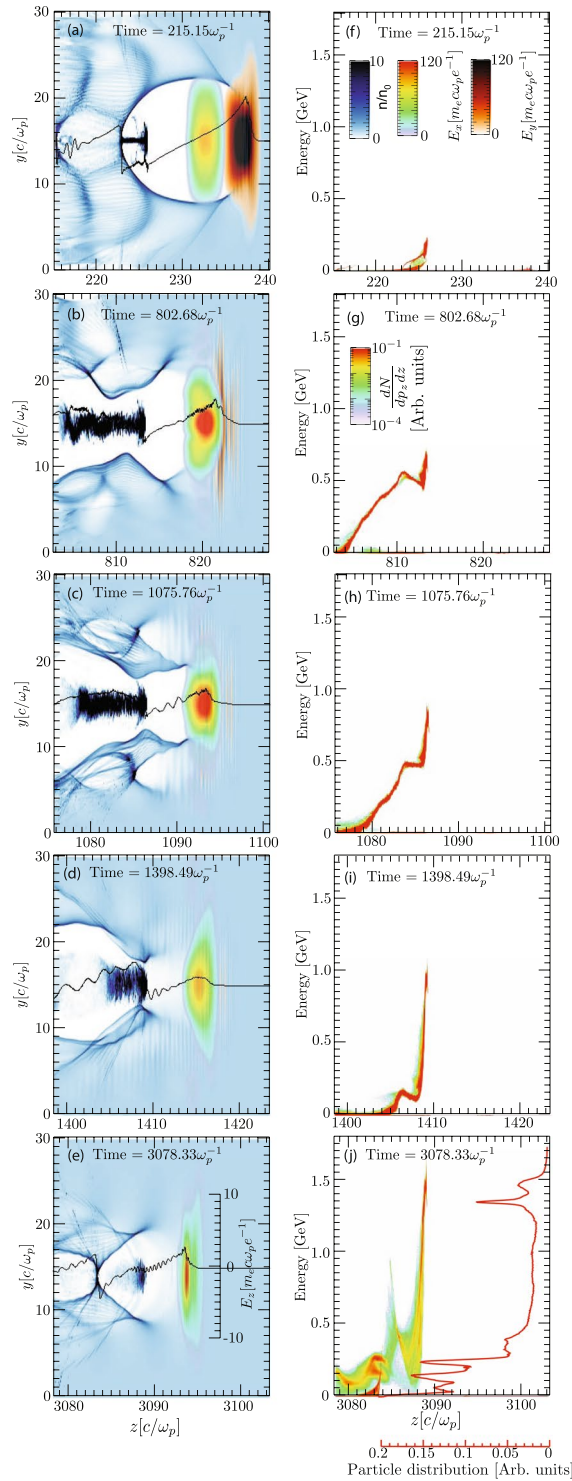
Figure 1. Proof-of-principle 3D PIC simulation. (**a**–**e**) Show the snapshots of laser fields and electron density distribution in the y-z plane at different times, and (**f**–**j**) show the energy-space distribution of accelerated electrons at respective times. The line in figures (**a**–**e**) is the longitudinal electric field (E_z) on the laser axis. The red line in figure (**j**) represents energy spectrum of the electrons showing bunched electron beam around 1.4 GeV.

in panel (j). In electron energy spectrum we observe two quasi-mono-energetic peaks, one at 1.3 Gev with 2.4% full-width-half maximum energy spread, and another peak at 1.5 GeV with 6.7% energy spread. At the same time the beam divergence and emittance reduces to 4 mrad and 10 mm mrad respectively in the second stage. Thus, the proposed all optical staged LWFA has potential to increase the energy by a factor of 3, and reducing

beam divergence and emittance, while the beam charge reduces. According to our analytical scaling [Eq. 2], the maximum energy gain for the total combined laser power of 215 TW, 800-nm fundamental wavelength and plasma density of 7.75×10^{18} cm^{-3}, is 1.4 GeV that is very close to the final energy of 1.5 GeV obtained in the 3D PIC simulations, showing 3 times energy enhancement as compared to the energy obtained in the single stage LWFA. As clear from Fig. 1(e), the acceleration length in the second stage is limited by the dephasing of energetic electrons in the wake of the second stage and, as a result, quasi-mono-energetic electrons at 1.4 GeV are produced [Fig. 1: panel (j)].

In order to obtain the necessary condition for the coupling of electron beam to the second stage, the case of LWFA in the matched regime[9] is considered with spherical and stationary nonlinear wakefields. The group velocity of the leading laser pulse is $v_{g1} \approx c[1 - (3/2)(\omega_p^2/\omega_0^2)]$ because of localized etching[9,32], and the following second harmonic laser pulse propagating within the first-stage bubble has group velocity $v_{g2} \approx c$. As a result, by the end of the first stage the distance between the two pulses reduces to $L_d = ct_d - (3/2)c\tau_{L(\omega_0)}$. During this time the leading part of the electron bunch, propagating with velocity c, also covers a distance $L_b = \left(\frac{3}{2}\right)c\tau_{L(\omega_0)}$ and, thus, the distance between the SL and the electron bunch stays constant in the first stage.

Role of time delay on the acceleration.   With these constraints, we can estimate the required time delay between FL and SL for the coupling. The lower limit of time delay is limited by two conditions; (i) for proper guiding SL must avoid the interaction with the remnant of the density pile-up created by the FL at its front; thus, $t_d > \left(\frac{3}{2}\right)\tau_{L(\omega_0)}$, and (ii) electrons accelerated in the first stage must reach the back of the bubble excited in the second stage, i.e. $L_b \geq 2(R(\omega_0) - R(2\,\omega_0)) - L_d$, which gives $t_d \geq 4(\sqrt{a_{0(\omega_0)}} - \sqrt{a_{0(2\omega_0)}})/\omega_p$. The upper limit of time delay again can be obtained from two conditions: (i) at the time of injection in the first stage the electron should not interact with the tail of the SL to avoid degradation in the beam-emittance, i.e. $t_d < (4\sqrt{a_{0(\omega_0)}} - \tau_{L(\omega_0)})/\omega_p$, and (ii) when coupled into the second stage the electrons should not already fall into the dephasing region of the second-stage-bubble, i.e. $t_d < 4(\sqrt{a_{0(\omega_0)}} - 0.5\sqrt{a_{0(2\omega_0)}})/\omega_p$. Thus, the suitable condition for choosing time delay for the coupling can be written as,

$$\text{Min}\left[4\left(\sqrt{a_{0(\omega_0)}} - 0.5\sqrt{a_{0(2\omega_0)}}\right),\ 4\sqrt{a_{0(\omega_0)}} - \tau_{L(2\omega_0)}\right]$$
$$> \omega_p t_d > \text{Max}\left[1.5\omega_p\tau_{L(\omega_0)},\ 4\left(\sqrt{a_{0(\omega_0)}} - \sqrt{a_{0(2\omega_0)}}\right)\right] \tag{3}$$

Including the effect of time delay, the acceleration length of second stage modifies to $L_{s2} = (8/3)(\omega_0^2/\omega_p^2)(4\sqrt{a_{0(\omega_0)}} - 2\sqrt{a_{0(2\,\omega_0)}} - \omega_p t_d)\,c/\omega_p$, and thus the energy gain in the second stage can be given in details by $\Delta E_{s2} = (8/3)mc^2 a_{0(2\,\omega_0)}(\omega_0^2/\omega_p^2)(2\sqrt{a_{0(\omega_0)}/a_{0(2\,\omega_0)}} - \omega_p t_d/(2\sqrt{a_{0(2\,\omega_0)}}))$.

To verify the role of time delay between the two pulses on the coupling of the electrons from the first stage into the second stage, we further perform a set of 2D simulations with two-color laser pulses of $P_{in} = 210$ TW and $\alpha = 0.33$ propagating in a 1.5-cm plasma with density 4.35×10^{18} cm^{-3}. The simulation box has dimensions of 25 $c/\omega_p \times 40\ c/\omega_p$ and is divided into 4800×400 cells, along z and x direction respectively, with 9 particles per cell. We consider FL parameters as: $a_{0(\omega_0)} = 5$, $\omega_0 = 20\ \omega_p$, $W_{0(\omega_0)} = 7\ c/\omega_p$ and $\tau_{L(\omega_0)} = \frac{\lambda_p}{2}$, and the SL parameters as: $a_{0(2\omega_0)} = 2.5$, $W_{0(2\omega_0)} = 5\ c/\omega_p$ and $\tau_{L(2\omega_0)} = \frac{\lambda_p}{2}$. Though the laser parameters are not exactly in the matched regime[9], the robustness of the proposed scheme can be tested. As shown in Fig. 2(a), the maximum energy can be optimized by manipulating the time delay between the two pulses. We observe that for $t_d \approx 1.8\tau_L$ the peak energy of 3.6 GeV is obtained after the end of second stage. For smaller time delays our simulations showed no coupling of the accelerated electron from the first stage into the second stage. As we further increase the time delay between the two pulses the effective acceleration length and hence the energy of the trapped electrons in the second stage decreases due to dephasing, as evident from Fig. 2(a) for $t_d > \frac{6}{\omega_p}$. We also perform a series of 2D PIC simulations to compare the dual stage LWFA driven by two single-frequency pulses (SFTP) with the dual stage driven by the two frequencies two pulse (TFTP). The details are provided in the supplementary material.

10 GeV electron beam driven by 0.6-PW laser.   As discussed before, one of the benefits of the two color dual stage LWFA is significant enhancement in the energy of an accelerated electron bunch, with Eq. (2) suggesting the realization of 10-GeV electron bunch. Keeping that in mind, we perform 2D PIC simulations using OSIRIS[23,24], and the results are summarized in Fig. 3. We consider equally energetic FL and SL with total laser energy of 30 J and each with 50-fs pulse-length, which corresponds to $P_{in} = 0.6$ PW. The other FL and SL parameters are: $a_{0(\omega_0)} = 5.38$, $\omega_0 = 40\ \omega_p$, $W_{0(\omega_0)} = 2\sqrt{a_{0(\omega_0)}}c/\omega_p$, $\tau_{L(\omega_0)} = \frac{\lambda_p}{2}$, $a_{0(2\omega_0)} = 3.4$, $W_{0(2\omega_0)} = 2\sqrt{a_{0(2\omega_0)}}c/\omega_p$, $\tau_{L(2\omega_0)} = \frac{\lambda_p}{2}$ and $t_d = 4.5\ /\omega_p$. To ensure guiding of the SL for a long distance in the second stage, a parabolic plasma channel profile $n = n_0\left[1 + \left(\frac{\Delta n_c}{n_0}\right)x^2\right]$ is considered with $\Delta n_c/n_0 = (4/W_{0(2\omega_0)}^4)(c/\omega_p)^2$ [2,9] and $n_0 = 1 \times 10^{18}$ cm^{-3}. The acceleration with a single laser pulse of energy 30 J and wavelength 0.8 μm is limited to 5 GeV (the dashed line in Fig. 3) after propagating 2.5-cm plasma due to dephasing. For the two-color dual-stage acceleration, the electron acceleration, after reaching 5 GeV in 2.5-cm plasma, is enhanced to 10 GeV with 20-pC charge in the second stage (the solid line in Fig. 3) within 8-cm plasma.

This is a significant improvement as compared to the single-stage LWFA. Lu et al.[9] scaling in the matched regime indicates that to generate 10-GeV electron beam in a 10-cm plasma with density 6×10^{17} cm^{-3} a 10-PW laser pulse is required. On the contrary, in two-color dual-stage LWFA, if the guiding of the second harmonic laser pulse is insured, 10-GeV electron beam is obtained in the same plasma length with an order of magnitude lower laser power. On the other hand, to generate 10-GeV electron bunch in single stage LWFA at lower laser power of 1PW, the laser
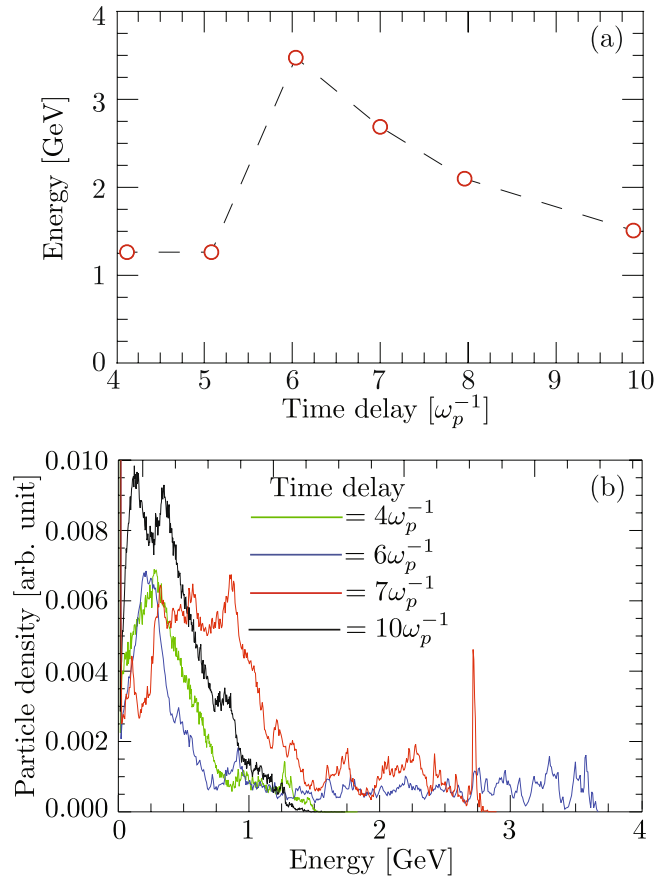
Figure 2. Effect of time-delay between the leading and trailing laser pulse on the electron energy. (**a**) Variation in the maximum energy with the time delay, and (**b**) spectrum of accelerated electrons by TFTP with time delay $\omega_p t_d = 4$ (green), 6 (blue), 7 (red), and 10 (black). The results are obtained with 2D PIC simulations.
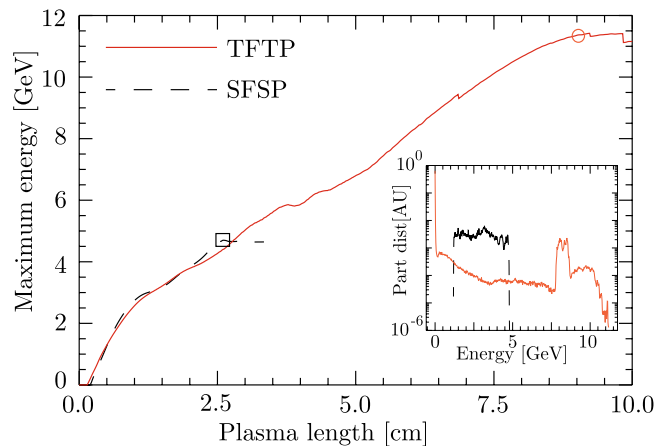

Figure 3. Time evolution of maximum energy of the accelerating electron bunch with 1PW laser. The solid line shows the energy gain from the TFTP, while the dashed line represents the energy gain from the single frequency single pulse (SFSP). The inset shows the electron spectra for the two cases at the plasma position of the maximum energy (⊙: *TETP*, ⊡: *SFSP*). The results are obtained with 2D PIC simulations.

pulse needed to be externally guided through a 1-m long plasma channel with on-axis density of $2 \times 10^{17}\,cm^{-3}$. Similarly, Vay et al.[33] have also shown the possibility of obtaining 10-GeV electron bunch from a 40-J laser pulse, externally guided through a 1.5-m-long plasma channel with on-axis $1 \times 10^{17}\,cm^{-3}$ plasma density. In comparison we have shown that two-color dual-stage LWFA can deliver same energies in one-order shorter plasma length. It is worth to mention the concerns on the transverse offset between the two pulse and plasma guiding structure. Such

transverse offsets may lead to transverse oscillations of the laser in the plasma channel[34,35], which can degrade the electron beam parameters, while it at the same can also lead to compact tunable polarized X-ray sources[35].

Conclusion

In conclusion, we have shown the feasibility of all optical two-color dual-stage LWFA with the help of multi-dimensional PIC simulations to obtain multi-GeV quasi-mono-energetic electron bunches. Two-color dual-stage LWFA yields higher acceleration energies, while keeping the quasi-mono-energetic property of the electron bunch, as compared to the same-energy single-pulse LWFA. We further provide estimates on the effect of the time delay between the two pulses on the acceleration process and show that, by fine-tuning the time delay and thus modifying the dephasing length in the second stage, the bunch energy and its quality can be optimized. We demonstrate that the two-color dual-stage LWFA can produce 10-GeV electron beam with an input power of 0.6 PW, which brings us closer to one of the milestones of LWFA.

References

1. Tajima, T. & Dawson, J. M. Laser electron accelerator. *Phys. Rev. Lett* **4**, 267–270 (1979).
2. Esarey, E., Sprangle, P., Member, S., Krall, J. & Ting, A. Overview of Plasma-Based Accelerator Concepts. *IEEE Trans. Plasma Sci.* **24**, 252–288 (1996).
3. Faure, J. *et al.* A laser-plasma accelerator producing monoenergetic electron beams. *Nature* **431**, 541–544 (2004).
4. Geddes, C. G. R. *et al.* High-quality electron beams from a laser wakefield accelerator using plasma-channel guiding. *Nature* **431**, 538–541 (2004).
5. Faure, J. *et al.* Controlled injection and acceleration of electrons in plasma wakefields by colliding laser pulses. *Nature* **444**, 737–739 (2006).
6. Korn, G., LeGarrec, B. & Rus, B. ELI Extreme Light Infrastructure Science and Technology with ultra-intense Lasers. In *CLEO:* 2013 CTu2D.7, https://doi.org/10.1364/CLEO_SI.2013.CTu2D.7 (2013).
7. Jeong, T. M. *et al.* Generation of high-contrast, 30 fs, 1.5 PW laser pulses. *Opt. Express* **20**, 10807 (2012).
8. Martins, S. F., Fonseca, R. A., Lu, W., Mori, W. B. & Silva, L. O. Exploring laser-wakefield-accelerator regimes for near-term lasers using particle-in-cell simulation in Lorentz-boosted frames. *Nat. Phys.* **6**, 311–316 (2010).
9. Lu, W., *et al.* Generating multi-GeV electron bunches using single stage laser wakefield acceleration in a 3D nonlinear regime. *Phys. Rev. Spec. Top. - Accel. Beams* **10**, 061301 (2007).
10. Leemans, W. & Esarey, E. Laser-driven plasma-wave electron accelerators. *Phys. Today* **62**, 44–49 (2009).
11. Pukhov, A. Strong field interaction of laser radiation. *Reports Prog. Phys.* **65**, R1–R55 (2002).
12. Lu, W., Huang, C., Zhou, M., Mori, W. B. & Katsouleas, T. Nonlinear theory for relativistic plasma wakefields in the blowout regime. *Phys. Rev. Lett.* **96**, 165002 (2006).
13. Vieira, J. & Mendonça, J. T. Nonlinear laser driven donut wakefields for positron and electron acceleration. *Phys. Rev. Lett.* **112**, 215001 (2014).
14. Sprangle, P., Tang, C. M. & Esarey, E. Relativistic self-focusing of short-pulse radiation beams in plasmas. *IEEE Trans. Plasma Sci.* **15**, 145–153 (1987).
15. Steinke, S. *et al.* Multistage coupling of independent laser-plasma accelerators. *Nature* **530**, 190–193 (2016).
16. Kim, H. T. *et al.* Enhancement of Electron Energy to the Multi-GeV Regime by a Dual-Stage Laser-Wakefield Accelerator Pumped by Petawatt Laser Pulses. *Phys. Rev. Lett* **111**, 165002 (2013).
17. Malka, V., Lifschitz, A., Faure, J. & Glinec, Y. Staged concept of laser-plasma acceleration toward multi-GeV electron beams. *Phys. Rev. Spec. Top. - Accel. Beams* **9**, 091301 (2006).
18. Kaganovich, D. *et al.* First demonstration of a staged all-optical laser wakefield acceleration First demonstration of a staged all-optical laser wakefield acceleration. *Phys. Plasmas* **12**, 100702 (2005).
19. Luo, J. *et al.* Multistage Coupling of Laser-Wakefield Accelerators with Curved Plasma Channel. *Phys. Rev. Lett* **120**, 154801 (2018).
20. Pollock, B. B. *et al.* Demonstration of a narrow energy spread, ~0.5 GeV electron beam from a two-stage laser wakefield accelerator. *Phys. Rev. Lett.* **107**, 045001 (2011).
21. Buck, A. *et al.* Shock-Front Injector for High-Quality Laser-Plasma Acceleration. *Phys. Rev. Lett* **110**, 185006 (2013).
22. Döpp, A. *et al.* Energy boost in laser wakefield accelerators using sharp density transitions. *Phys. Plasmas* **23**, 056702 (2016).
23. Fonseca, R. A. *et al.* In *Computational Science–ICCS* 2002: *International Conference Amsterdam*, *The Netherlands*, *April 21–24, 2002 Proceedings*, *Part III* (eds Sloot, P. M. A., Hoekstra, A. G., Tan, C. J. K. & Dongarra, J. J.) 342–351, https://doi.org/10.1007/3-540-47789-6_36 (Springer Berlin Heidelberg, 2002).
24. Fonseca, R. A. *et al.* One-to-one direct modeling of experiments and astrophysical scenarios: pushing the envelope on kinetic plasma simulations. **50**, 124034 (2008).
25. Pathak, V. B., Vieira, J., Fonseca, R. A. & Silva, L. O. Effect of the frequency chirp on laser wakefield acceleration. *New J. Phys.* **14**, 023057 (2012).
26. Kalmykov, S. Y., Beck, A., Davoine, X., Lefebvre, E. & Shadwick, B. A. Laser plasma acceleration with a negatively chirped pulse: all-optical control over dark current in the blowout regime. *New J. Phys.* **14**, 033025 (2012).
27. Kim, H. T. *et al.* Stable multi-GeV electron accelerator driven by waveform-controlled PW laser pulses. *Sci. Rep.* **7**, 10203 (2017).
28. Zeng, M. *et al.* Multichromatic narrow-energy-spread electron bunches from laser-Wakefield acceleration with dual-color lasers. *Phys. Rev. Lett.* **114**, 084801 (2015).
29. Xu, X. L. *et al.* Nanoscale Electron Bunching in Laser-Triggered Ionization Injection in Plasma Accelerators. *Phys. Rev. Lett.* **117**, 034801 (2016).
30. Tzoufras, M., Tsung, F. S., Mori, W. B. & Sahai, A. A. Improving the self-guiding of an ultraintense laser by tailoring its longitudinal profile. *Phys. Rev. Lett.* **113**, 245001 (2014).
31. Kalmykov, S. Y., Davoine, X., Lehe, R., Lifschitz, A. F. & Shadwick, B. A. Optical control of electron phase space in plasma accelerators with incoherently stacked laser pulses. *Phys. Plasmas* **22**, 056701 (2015).
32. Decker, C. D., Mori, W. B., Tzeng, K.-C. & Katsouleas, T. The evolution of ultra-intense, short-pulse lasers in underdense plasmas. *Phys. Plasmas* **3**, 2047 (1996).
33. Vay, J. L. *et al.* Modeling of 10 GeV-1 TeV laser-plasma accelerators using Lorentz boosted simulations. *Phys. Plasmas* **18**, 123103 (2011).
34. Pathak, V. B., Vieira, J., Silva, L. O. & Nam, C. H. Laser dynamics in transversely inhomogeneous plasma and its relevance to wake field acceleration. *Plasma Phys. Control. Fusion* **60**, 054001 (2018).
35. Luo, J. *et al.* A compact tunable polarized X-ray source based on laser-plasma helical undulators. *Sci. Rep.* **6**, 1–8 (2016).

Acknowledgements

Author Contributions

V.B.P. and H.T.K. proposed the concept. V.B.P. developed the theory and performed the simulations. H.T.K. and C.H.N. supervised the physical interpretations. All authors contributed to interpret physical process and write the paper.

Additional Information

Supplementary information accompanies this paper at https://doi.org/10.1038/s41598-018-30095-4.

Competing Interests: The authors declare no competing interests.

Publisher's note: Springer Nature remains neutral with regard to jurisdictional claims in published maps and institutional affiliations.